

# Optimization of Mounting Methods for Tension-Compression Testing of Murine Intervertebral Disc Joints

Joanna E. Veres, Shiyin Lim, Grace D. O'Connell  
Research Sponsor: Grace O'Connell (Dept. of Mechanical Engineering)

**MAJOR, YEAR, DEPARTMENTAL:** Bioengineering and Chinese, Fourth Year, Department of Bioengineering

## ABSTRACT

Murine models are an invaluable tool for studying intervertebral disc biology and degeneration, but mechanically testing the small discs proves challenging. Current methods may require expensive custom test jigs or are not detailed enough to replicate in other research labs. Thus, assessing the material properties of the murine disc requires the creation of lab-specific sample mounting and test methods. In this study, we aimed to develop a widely applicable sample mounting protocol for mechanical testing of murine intervertebral disc joints. We designed and tested five different sample mounting methods, ranked the relative success of each method based on six predetermined criteria, and selected the most promising method for further evaluation. The SAM Box V3 was the best of these methods with seven tested samples passing all six criteria. The findings of this study suggest that the SAM Box V3 is a reliable sample mounting method for mechanically testing murine intervertebral disc joints that is inexpensive, widely applicable, and open source.

## INTRODUCTION

The intervertebral disc (IVD) is the soft tissue found between vertebrae that gives the spine greater flexibility, distributes mechanical loads, and dissipates energy.<sup>1</sup> The disc consists of two main parts: the nucleus pulposus (NP) and annulus fibrosus (AF)<sup>1</sup>(Fig 1). The NP is a central, gelatinous structure composed of cells populating a collagen, proteoglycan (core protein with attached glycosaminoglycan groups) matrix that holds and moves water around to allow for flexibility.<sup>2</sup> The AF is a series of concentric collagenous rings containing parallel collagen fiber bundles and elastin fibers that hold the NP together.<sup>2</sup> Additionally, on the superior and

inferior ends of the disc are cartilage endplates.<sup>3</sup> These thin layers of hyaline cartilage act both as a mechanical barrier and gateway for nutrient transport into the disc.<sup>3</sup>

Disc degeneration is a broad diagnosis, characterized by IVD damage through natural age-related wear that often causes pain, limits mobility, and negatively impacts quality of life.<sup>4</sup> Hallmarks of disc degeneration include increased disc stiffness, loss of proteoglycan content, and disorganization of collagen fibers; all which are tied to changes in biomechanical function.<sup>4</sup> Given that approximately 40% of adults over age 40 and 80% of people over 80 have some degree of disc degeneration,<sup>5</sup> and that disc degeneration is strongly linked to biomechanics,<sup>6</sup> disc

mechanics is a popular topic of study. As human discs are expensive, not easily accessible, and subject to high variability due to variations in lifestyle, animal models are often used in place of human samples in disc mechanics research.<sup>7</sup>

Mice are a commonly used animal model for studying the degeneration or regeneration of disc health because their discs

are biochemically and mechanically similar to human discs, and they can be easily genetically manipulated.<sup>7</sup> However, due to their small size and high sensitivity to changes in position and environment, assessing the material properties of mouse discs can be challenging. In the literature, current methods of testing murine discs require expensive custom jigs<sup>8,9,10</sup> or are not detailed enough to replicate

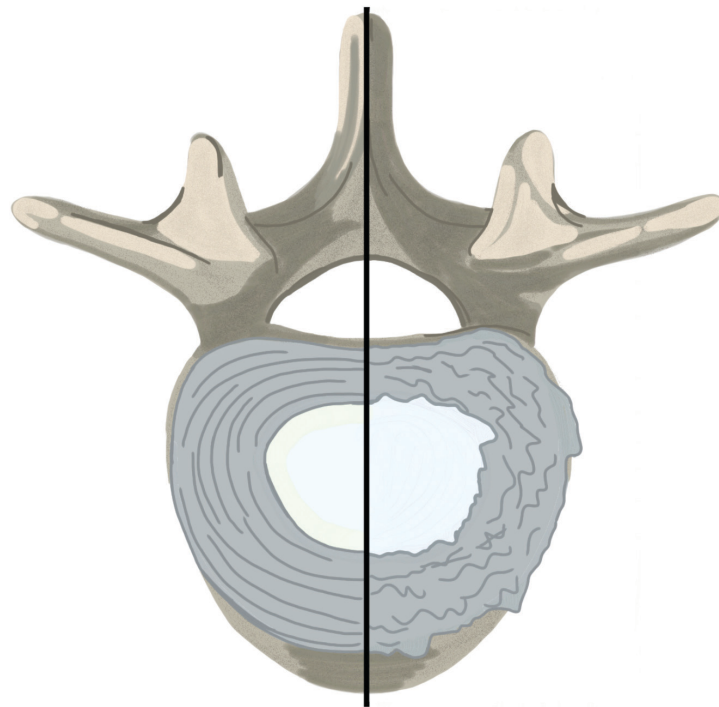


**Figure 1:** A representation of a healthy (left half) and degenerated (right half) intervertebral disc.

the methods used,<sup>11</sup> making it difficult and expensive to conduct these tests.

The objective of this study was to create an inexpensive, open-source method to mechanically test murine discs that was repeatable across samples and kept the disc as close to physiological alignment and tissue hydration as possible.

## METHODS

### GEOMETRY COLLECTION

Lumbar columns (L1-L5) were acquired from mice through a sample-sharing program at UC Berkeley. The spines were stored at -20°C prior to thawing for computed tomography (CT) scanning. The columns were scanned at 0.092 mm resolution. To find disc height, the CT scans were rotated and measured in

DataViewer (vers. 1.5.6.2), with triplicate measurements of disc height in the midcoronal and midsagittal planes averaged to calculate a single disc height. To calculate disc area, cross-sectional images of the vertebral endplates were taken in CTvox (vers. 3.3.0 r1403) and disc area was measured as the area of the endplate using ImageJ (vers. 1.52q) (Fig 2).

### SAMPLE PREPARATION

Preparation consisted of tissue removal from the lumbar column to expose the discs. Cuts were made through the transverse plane of the L1/2 and L3/4 discs. Finally, the posterior bony processes were removed, leaving an L2/3 and an L4/5 bone-disc-bone motion segment (Fig 3).

### MECHANICAL TESTING

Mechanical testing was conducted on an Instron 5943 Series Universal Testing System (Illinois Tool Works Inc., Norwood, MA) and consisted of twenty cycles of tension-compression between -1.0N and +1.0N. All samples were mounted according to one of the variable mounting techniques described below, then loaded into the Instron with the clamp ends fixed. In the final mounting protocol, samples were hydrated for 15 minutes in saline polyethylene glycol (sPEG) before testing.<sup>13</sup> A 17% wt/vol concentration sPEG was used to prevent the tissue from overhydrating before testing. The neutral zone (NZ), compressive, and tensile stiffness were measured and normalized to specimen geometry. Compressive and tensile stiffnesses

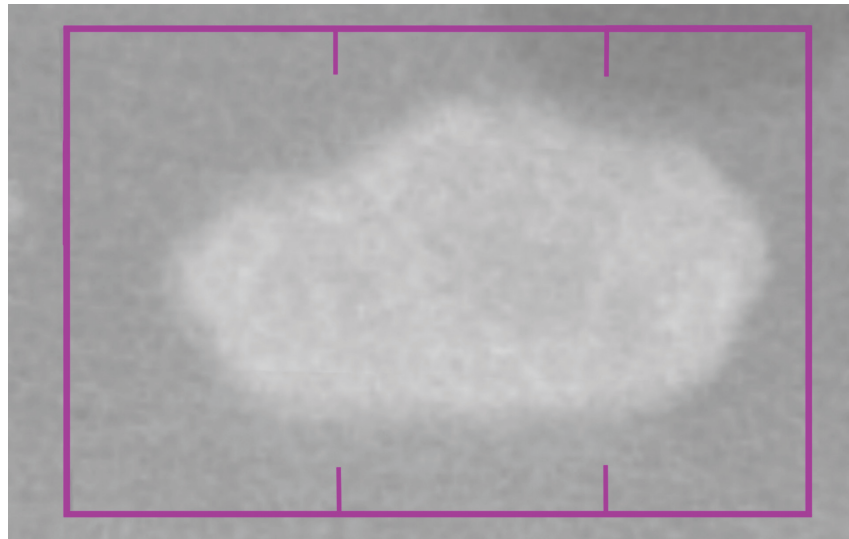


**Figure 2: An example cross sectional, superior transverse plane reconstruction screen shot from CTvox with a scaling tic marks (1mm).**

were calculated by curve fitting for data between 80-100% of the maximum applied load (Figure 4A – red lines), and the NZ was determined using the double sigmoid curve-fit method (Figure 4B – blue line).<sup>14</sup> Data will be presented as mean±standard deviation.

### SUCCESS CRITERIA

The relative success of each mounting method was based on six criteria: 1) the transverse plane of the disc remained parallel to the applied load, 2) the disc was kept in a physiologically neutral position, 3) the sample was not damaged, 4) the sample remained fixed in the mount, 5) the disc stayed hydrated during testing, and 6) a tertiary load-displacement curve was observed and repeatable.

### SANDPAPER MOUNTING METHODS

The first sample fixation method consisted of fixing each vertebral body between two sheets of sandpaper with cyanoacrylate (n=6, Figure 5A). The second sample fixation method was identical to the first, but polymethyl methacrylate (PMMA) was used instead of cyanoacrylate (n=7, Figure 5B).

### SAM BOX MOUNTING METHODS

The third method introduced the first iteration of the Sample Aligning Mechanical testing Box (SAM Box). For SAM Box Version 1 (V1), the sample was potted in PMMA in 3D printed pieces connected with thin bridges. After the PMMA was cured, the bridges were cut, allowing for each side of the joint segment

to articulate separately (Figure 5C). The 3D printed pieces were then loaded into the Instron clamps (n=7).

The second iteration of the SAM Box (SAM Box V2; Figure 5D) removed the alignment bridges, instead relying on clamps and the Instron to pot samples directly in their testing configuration (n=6). However, PMMA curing times in the testing configuration led to tissue dehydration prior to testing.

The third iteration of the SAM Box (SAM Box V3) added a bath around the sample, allowing for a fifteen minute hydration period after PMMA curing, prior to sample testing (n=7, Figure 5E).

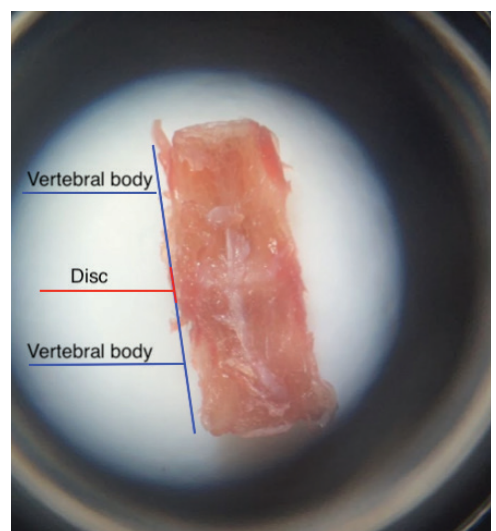


**Figure 3: A fully prepped lumbar joint segment before potting (shown through a dissecting scope).**

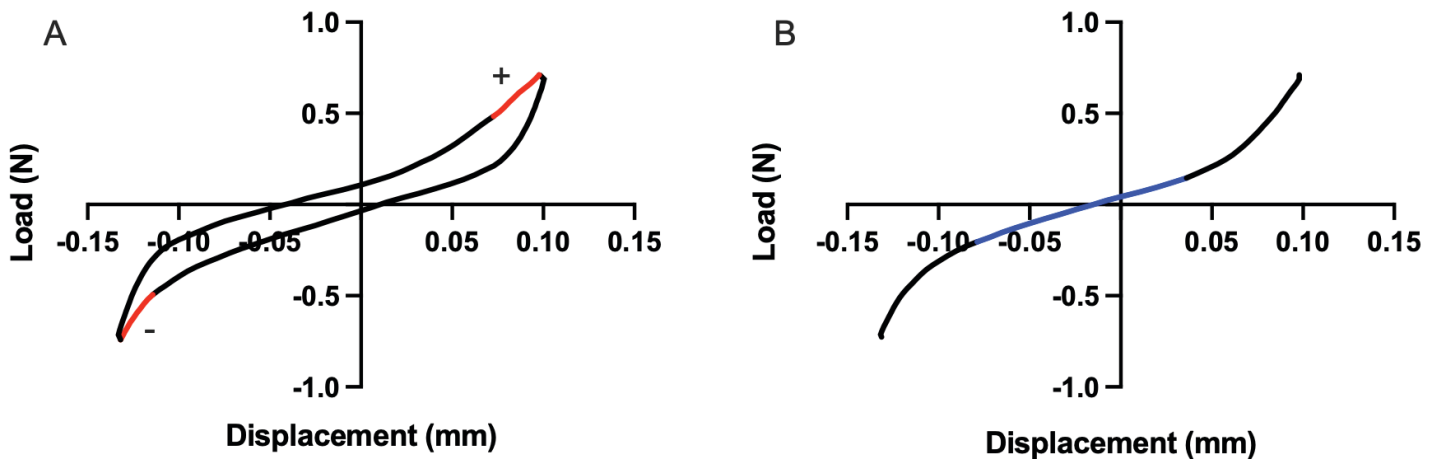


Figure 4: Representative axial-tension compression curves with tensile and compressive stiffnesses and neutral zone highlighted.

## RESULTS

### FAILED METHODS

The sandpaper cyanoacrylate method failed four out of six samples tested. Using this method, the sample did not remain fixed to the sandpaper during testing, parallel alignment was highly variable, and cyanoacrylate often seeped onto the disc. To address this, PMMA was used instead of cyanoacrylate, which limited seeping

and created rigid fixation to the sandpaper. However, the sandpaper PMMA method still failed five out of seven samples. Using the sandpaper and PMMA, parallel alignment was difficult and highly variable. To improve sample alignment, the SAM Box V1 was used to orient samples during potting, which retained rigid fixation and physiological alignment. But, because samples were potted prior to testing, the mounting process often

applied unwanted bending or torsional stresses on the joint segment. This led to failure of seven out of twelve samples. Next, samples were potted in place on the Instron using the SAM Box V2 method. This addressed the alignment difficulties, kept rigid fixation, and protected the disc from extraneous glue. However, the added drying time led to four out of six samples failing.

### THE SAM BOX V3

The SAM Box V3 was the most successful prototype with the success criteria being met for all 7 samples. The added bath of the SAM Box V3 allowed for tissue rehydration prior to testing. This method was easy to use, kept samples hydrated and aligned, and consistently produced load displacement curves that agreed well with data reported in the literature.

Axial compression-tension mechanics were measured with SAM Box V3. The normalized NZ stiffness was  $0.238 \pm 0.138$  MPa, normalized compressive stiffness was  $4.177 \pm 1.487$  MPa, and normalized tensile stiffness was  $2.830 \pm 1.271$  MPa (Figure 6).

## DISCUSSION

The SAM Box V3 is a mounting method for murine lumbar disc joints that is easy to use, inexpensive, and mimics physiological conditions. Each SAM Box V3 costs about \$1.00 in polylactic acid filament and takes about an hour to print on an Ultimaker 3.

The results presented here align well with published results. Sarver et al. reported

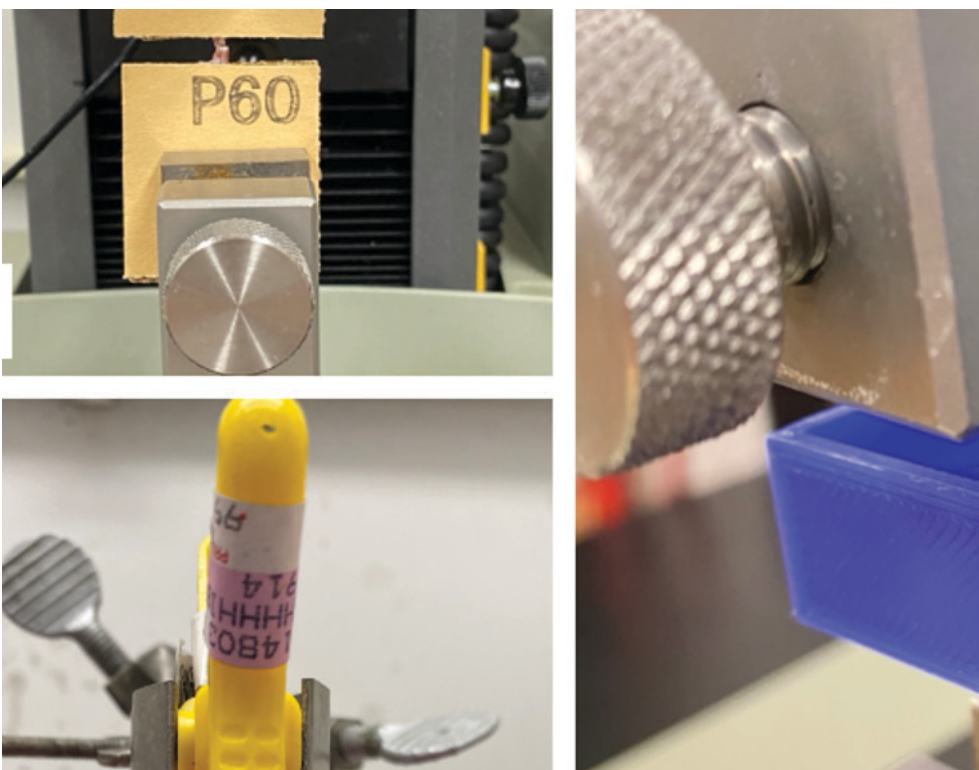


Figure 5: Sample mounting methods. A, B) Cyanoacrylate and PMMA sandpaper methods, C-E) SAM Box Versions 1-3 (V1-V3).

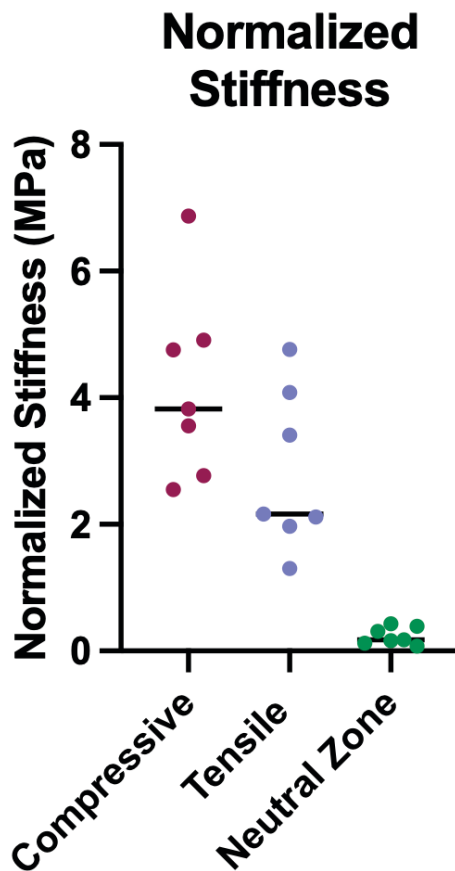


Figure 6: Normalized stiffnesses from SAM Box V3 pilot testing.

a normalized NZ stiffness of  $0.58 \pm .45$ MPa, a normalized compressive stiffness of  $3.65 \pm 0.98$ MPa, and a normalized tensile stiffness of  $2.54 \pm 0.44$ MPa.<sup>14</sup> Additionally, Choi et al. reported a normalized compressive stiffness of  $5 \pm 0.5$ MPa using a similar test protocol.<sup>15</sup> These results suggest that the SAM Box V3 method is consistent with other methods used in the field, while being easy to use, comparatively cheaper, and more adaptable to different fixturing methods.

Despite the consistent results presented here, there are limitations to the SAM Box V3. First, testing was performed at room temperature rather than body temperature ( $37^{\circ}\text{C}$ ). However, we chose to test at room temperature to better match methods used in the literature for comparison. Additionally, adding 3D-printed fixtures to the load chain may result in an increase in machine compliance, which needs to be accounted for when analyzing mechanical test data. However, because the applied loads are minimal (approx. 1N), it is unlikely that the 3D-printed boxes will experience large

deformations.

Overall, the SAM Box V3 allows for easy mounting, gripping, and testing of murine disc joint segments while maintaining hydration and alignment. It is a low-cost method that can be applied in tensile-compression mechanical tests, which is important for studying disc mechanics with degeneration, injury, or regeneration.

#### ACKNOWLEDGEMENTS

This study was supported by the UC Berkeley SURF Program.

#### REFERENCES

- Erwin, W. M., & Hood, K. E. (2014). The cellular and molecular biology of the intervertebral disc: A clinician's primer. *The Journal of the Canadian Chiropractic Association*, 58(3), 246–257.
- Adams MA, Roughley PJ. What is intervertebral disc degeneration, and what causes it? *Spine (Phila Pa 1976)*. 2006 Aug 15;31(18):2151-61. doi: 10.1097/01.brs.0000231761.73859.2c. PMID: 16915105.
- Moon, S. M., Yoder, J. H., Wright, A. C., Smith, L. J., Vresilovic, E. J., & Elliott, D. M. (2013). Evaluation of intervertebral disc cartilaginous endplate structure using magnetic resonance imaging. *European spine journal : official publication of the European Spine Society, the European Spinal Deformity Society, and the European Section of the Cervical Spine Research Society*, 22(8), 1820–1828. <https://doi.org/10.1007/s00586-013-2798-1>
- Dydyk AM, Ngnitewe Massa R, Mesfin FB. Disc Herniation. [Updated 2021 Jul 12]. In: StatPearls [Internet]. Treasure Island (FL): StatPearls Publishing; 2022 Jan-. Available from: <https://www.ncbi.nlm.nih.gov/books/NBK441822/>
- Medical Advisory Secretariat (2006). Artificial discs for lumbar and cervical degenerative disc disease -update: an evidence-based analysis. *Ontario health technology assessment series*, 6(10), 1–98.
- Hong, C., Lee, C. G., & Song, H. (2021). Characteristics of lumbar disc degeneration and risk factors for collapsed lumbar disc in Korean farmers and fishers. *Annals of occupational and environmental medicine*, 33, e1
- <https://doi.org/10.35371/aoem.2021.33.e16>
- Jin, L., Balian, G., & Li, X. J. (2018). Animal models for disc degeneration-an update. *Histology and histopathology*, 33(6), 543–554. <https://doi.org/10.14670/HH-11-910>
- Torre, O. M., Das, R., Berenblum, R. E., Huang, A. H., & Iatridis, J. C. (2018). Neonatal mouse intervertebral discs heal with restored function following herniation injury. *FASEB journal : official publication of the Federation of American Societies for Experimental Biology*, 32(9), 4753–4762. <https://doi.org/10.1096/fj.201701492R>
- Jeannie F. Bailey, Alan R. Hargens, Kevin K. Cheng, Jeffrey C. Lotz, Effect of microgravity on the biomechanical properties of lumbar and caudal intervertebral discs in mice, *Journal of Biomechanics*, Volume 47, Issue 12, 2014, Pages 2983-2988, ISSN 0021-9290, <https://doi.org/10.1016/j.jbiomech.2014.07.005>.
- Elliott, D. M., & Sarver, J. J. (2004). Young investigator award winner: validation of the mouse and rat disc as mechanical models of the human lumbar disc. *Spine*, 29(7), 713–722. <https://doi.org/10.1097/01.brs.0000116982.19331.ea>.
- Boxberger, J. I., Sen, S., Yerramalli, C. S., & Elliott, D. M. (2006). Nucleus pulposus glycosaminoglycan content is correlated with axial mechanics in rat lumbar motion segments. *Journal of orthopaedic research : official publication of the Orthopaedic Research Society*, 24(9), 1906–1915. <https://doi.org/10.1002/jor.20221>
- Werbner, B., Lee, M., Lee, A., Yang, L., Habib, M., Fields, A. J., & O'Connell, G. D. (2022). Non-enzymatic glycation of annulus fibrosus alters tissue-level failure mechanics in tension. *Journal of the*

- mechanical behavior of biomedical materials, 126, 104992. <https://doi.org/10.1016/j.jmbbm.2021.104992>
13. Smit, T.H., van Tunen, M.S., van der Veen, A.J. et al. Quantifying intervertebral disc mechanics: a new definition of the neutral zone. *BMC Musculoskelet Disord* 12, 38 (2011). <https://doi.org/10.1186/1471-2474-12-38>
  14. Sarver, J.J. and Elliott, D.M. (2005), Mechanical differences between lumbar and tail discs in the mouse. *J. Orthop. Res.*, 23: 150-155. <https://doi.org/10.1016/j.orthres.2004.04.010>
  15. Choi, H., Tessier, S., Silagi, E. S., Kyada, R., Yousefi, F., Pleshko, N., Shapiro, I. M., & Risbud, M. V. (2018). A novel mouse model of intervertebral disc degeneration shows altered cell fate and matrix homeostasis. *Matrix biology : journal of the International Society for Matrix Biology*, 70, 102–122. <https://doi.org/10.1016/j.matbio.2018.03.019>